Aqeel *et al.*
Future Journal of Pharmaceutical Sciences (2022) 8:32
https://doi.org/10.1186/s43094-022-00422-8

Future Journal of Pharmaceutical Sciences

RESEARCH Open Access

In silico approach for the development of phenolic derivatives as potential anti-angiogenic agents against lysyl oxidase-like 2 enzyme

Muhammad Tahir Aqeel[1,2*], Nisar-Ur-Rahman[1], Arif-ullah Khan[3], Zaman Ashraf[4], Samiullah Khan[2] and Muazzam Arif[5]

Abstract

Background: Lysyl oxidase-like 2 (LOXL2) has recently been explored as extremely pivotal protein involved in angiogenesis which results in metastasis of numerous types of cancers. Hence, LOXL2 is an exciting new target for drug development against tumor progression and its spread to distant organs. Newly synthesized derivatives of natural phenolic antioxidant guaiacol (T1 to T8) were evaluated for their potential as anti-angiogenic agents using in silico approach. The drug likeness properties and toxicity of the synthesized derivatives have also been determined. Active binding sites of LOXL2 protein were determined by online server DoGSiteScorer, and lead–target interactions and conformations of pose analysis were done by using AutoDock Vina and Discovery Studio 4.0. The GUSAR model was applied to find the toxicity and ADMET properties. On the other hand, the chemoinformatics prediction was also performed using online FAF Drug Server and Molinspiration online server.

Results: Lead molecules from T1 to T8 showed promising binding affinity values, especially T5 and T8 showed best fit in the binding pocket of target enzyme (binding energies − 7.9 and 8.0 kcal/Mol, respectively). The stability of docked complexes was further evaluated using molecular dynamic simulation studies using GROMACS force field, and both leads (T5 and T8) were found to be strongly bounded to the active binding sites. The ADMET results revealed that all experimental molecules were virtually nontoxic and showed compliance with rule of five.

Conclusion: The present work will further enable researchers to understand how computer-aided drug designing tools may help to expedite new drug discovery process in a minimum cost.

Keywords: Anti-angiogenic, Lysyl oxidase-like 2, Phenolic derivatives, MD simulation, *In silico*

Background

Cancer is a life-threatening disease and difficult to cure only because of its ability to spread to adjacent or distant organs. The cancer cells can penetrate and circulate in the lymphatic and intravascular system and then proliferate at another site, called metastasis. Micro-metastasis is a major reason for the reoccurrence of this fatal disease [1]. In physiology, new blood vessels are formed from the existing epithelium and is known to occur in humans at different stages of life, like during wound healing and reproduction, called angiogenesis and pathologically, in malignant tumor growth and metastatic cancer. Lysyl oxidase (LOX) family is believed to be a major multiple homologous enzyme series responsible for the new vascularization (angiogenesis) in spreading tumor [2].

*Correspondence: tahiraqeelmalik@gmail.com

[1] Department of Pharmacy, COMSATS University Islamabad, Abbottabad Campus, Islamabad 22060, Pakistan
Full list of author information is available at the end of the article

The LOX family is comprised of five paralogues: LOX and LOX-like 1–4 (LOXL1–4) and are secreted by copper-dependent amine oxidases. The LOX family is involved in maintaining the structural integrity and tensile strength of many tissues by covalently cross-linking elastin/or collagen in the extracellular matrix (ECM) [3]. During the normal conditions, the expressions of the LOX family are tightly controlled; however, in cancer and in many diseases related to ECM, the altered expression of the proteins responsible for this enzyme system has been reported. The chronic fibrosis resulting from the cross-linking of ECM is known as a driving force behind certain type of cancers, like liver cancer and hepatic fibrosis. There is scarcity of information about the linkage of LOX-mediated connective tissue disorders and cancer [4]. Apart from the cross-linking of ECM, these enzymes may also have other functional roles. The complex nature of these enzymes system is represented by a wide range of spatial and temporal expression as well as its inability to perform the functions of other enzymes of the family.

The family of LOX enzymes is secretive in its nature and attained much attention to be explored for their role in cancer. The involvement of activities of LOX family in the development of metastasis is thoroughly substantiated, and inhibition of LOX and LOX2 demonstrated a significant reduction in the metastasis [5].

In recent studies, there are strong pieces of evidence of the involvement of LOX family in the metastasis. For example, in head and neck squamous cell carcinoma (HNSCC) and in various other types of cancers, there was an increase in levels of LOX mRNA and protein, including breast [5, 6], colorectal [7, 8] and prostate cancer [9]. Also, the increased desmoplastic stroma exhibited an association with increased LOXL2 expression [10]. Importantly, there is rising evidence that high LOXL2 expression is associated with tumor grade, decreased survival and poor prognosis [11]. Recently, in primary gastric tumors the increased expression of LOXL2 is correlated with lymph node metastasis, tumor invasion and ultimately with poor prognosis. Moreover, the high LOXL2 expression has also been reported to cause more severe forms of breast cancers [12].

Phenolic compounds and their derivatives are well known and well studied for their variety of pharmacological distinctiveness such as anti-cancer, antioxidant, anti-inflammatory and cardio-protective [13]. Quercetin derivatives are another group of naturally derived phenolic derivatives; those are found to inhibit metastasis both in *in vitro* and in *in vivo* models [14]. Likewise, in various studies dietary phenolic compounds including carnosic acid, carnosol, ellagic acid, tyrosol and hydroxytyrosol have shown excellent anti-angiogenic potential during *in vitro* evaluation [15–17].

The guaiacol is a natural phenolic antioxidant and has been known for its health benefits. The guaiacol derivatives T1 to T8 shown in Fig. 1 used in this study have been synthesized in our laboratory and reported previously [18]. The scarcity of available resources for laboratory testing and the extensive consumption of chemicals makes drug discovery for cancer an expensive job. As an alternative strategy for new drug discovery, in silico drug designing is tremendously advantageous in terms of low cost, quick outcomes and at times it can address questions from researchers those are difficult to answer in the laboratory [18]. Active binding sites of LOXL2 protein were determined by online server DoGSiteScorer [19], and lead–target interactions and conformations of pose analysis were done by using AutoDock Vina [20] and Discovery Studio 4.0 [21]. The GUSAR model was applied to find the toxicity and ADMET properties [22]. On the other hand, the chemoinformatics prediction was performed using online FAF Drug Server [23] and Molinspiration online server [24].

Methods

Accession of 3D structure of target protein

The 3D structure of LOXL2 protein was obtained using homology modeling approach via I-Tasser online server [25]. Among the proposed models, the highest C score was used as selection criteria.

Preparation of target protein

The newly modeled protein structure was protonated using the AutoDock tools program [26], and thereafter the obtained structure was energy-minimized and saved in PDBQT format.

Preparation of ligands

The structures of phenolic lead molecules (T1 to T8) were drawn and energy-minimized in Discovery Studio 4.0 software [21] and saved in PDB format. For each compound, the most stable conformation was utilized in docking calculation and the AutoDock tools program [26] was used to generate the docking input files in PDBQT format.

Binding pocket

Protein structure was uploaded to an online server DoGSiteScorer [19] in PDB format in order to assess the most suitable binding pocket on the basis of druggability. The three-dimensional parameters of the most druggable binding pockets were used to dock lead compounds with the target proteins.

The grid box center values (center $x = -2.52$, center $y = 1.63$ and center $z = -10.33$) and size values (size

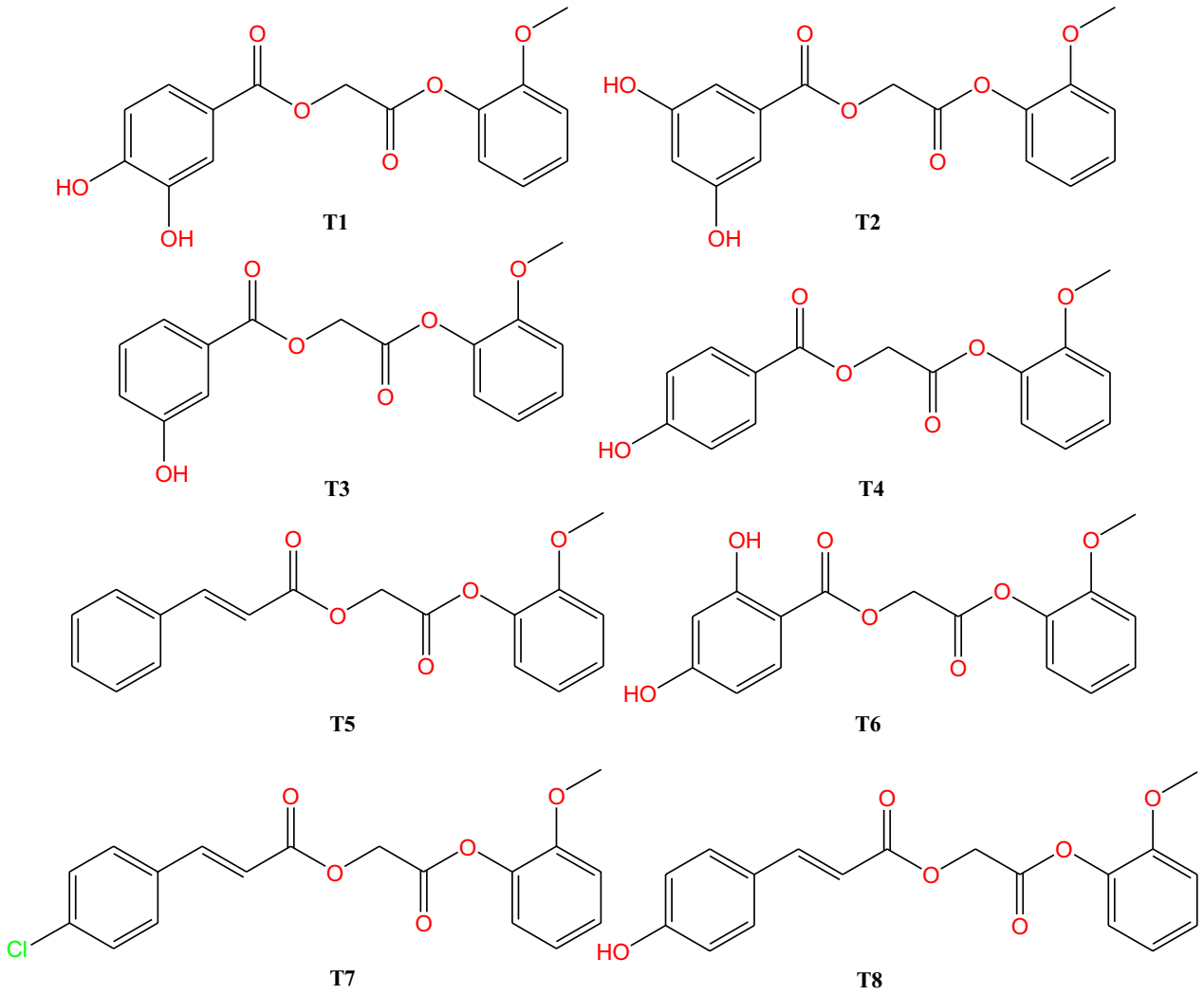

Fig. 1 Structures of synthetic phenolic derivatives (methoxyphenol derivatives) from T1 to T8

$x = 20$, size $y = 22$ and size $z = 32$) were used for better conformational position in the active region of LOXL2.

Chemoinformatic and pharmacokinetic prediction

All phenolic derivatives were screened for druglikeness properties including molecular weight, number of hydrogen bond donor atoms (HBD), number of hydrogen bond acceptor atoms (HBA), molar volume, topological polar surface area (TPSA), rigid and flexible bonds and water partition coefficient (log *P),* using online chemoinformatics drug database FAF Drug Server [23] and Molinspiration server (http://www.molinspiration.com//cgi-bin/properties) [24]. Additionally, solubility (mg/L) and solubility forecast index were also determined using the same online tools for all experimental phenolic derivatives.

Rat acute toxicity prediction

All phenolic derivatives were computationally screened for their possible rat acute toxicity prediction via four administration routes, including intraperitoneal (IP), intravenous (IV), oral and subcutaneous (SC), using general unrestricted structure–activity relationship (GUSAR) [22].

Docking studies

The PDB formats of all experimental phenolic derivatives were prepared and quality-treated to form PDBQT file using AutoDock tools [26]. Homology model of LOXL2 was built using I-Tasser online server [25]. Among five proposed models, one was selected based on C Score criteria. Based on the highest confidence scores (C Scores),

the best model was selected as the most stable model using I-Tasser online server.

All the lead molecules (T1–T8) were docked separately against LOXL with exhaustiveness value = 50 using AutoDock Vina software [20]. The predicted docked complexes were evaluated based on the lowest binding energy (kcal/mol) values, and the three-dimensional graphical depictions of all the docked complexes were accomplished by Discovery Studio 4.0 [21]. The two best docked molecules were subjected for molecular dynamic (MD) simulation.

Molecular dynamics (MD) simulations

The best docked energy (Kcal/mol) complexes (T5 and T8) were selected for MD simulations study. This study was performed by Groningen Machine for Chemicals Simulations (GROMACS) 4.5.4 package [27] with GROMOS 53A6 force field and water model SPC216 [28]. The topology files of receptor and ligand were created by using GROMOS 53A6 force field and online PRODRG Server [29]. The receptor–ligand complexes were then placed in the middle of cubic box with 0.9 Å distance. The energy minimization (n steps = 50,000) was done by steepest descent approach (1000 ps), and energy calculation was made by particle mesh Ewald (PME) method [30]. The final MD run was adjusted to 15,000 ps with n steps 7,500,000 and analyzed using Xmgrace software (http://plasma-gate.weizmann.ac.il/Grace/) [31, 32].

Results

Chemoinformatics

All phenolic lead derivatives complied with rule of five, with excellent aqueous solubility and good oral bioavailability. Table 1 refers to the chemoinformatic properties of phenolic derivatives, which clearly show that all phenolic derivatives from T1 to T8 possess good and acceptable physiochemical properties like molecular weight, flexibility, hydrogen bond donor, hydrogen bond acceptor, solubility and no violation of Lipinski rule.

Rat acute toxicity prediction

This test was performed to check the safety profile of these newly synthesized phenolic derivatives computationally by using GUSAR model (http://www.way2drug.com/gusar/acutoxpredict.html). The results showcased promising values of T1 (IP = 656,000 mg, IV = 215,400 mg, Oral = 3,081,000 mg, SC = 3,824,000 mg), T2 (IP = 637,800 mg, IV = 223,400 mg,

Table 1 Chemoinformatic properties of phenolic derivatives

Physicochemical Properties	T1	T2	T3	T4	T5	T6	T7	T8
Molecular weight	318	318	302	302	312	318	346	328
Logp	2.58	2.51	2.87	2.87	3.65	3.13	4.28	3.3
LogD	2.46	2.48	2.79	2.79	3.64	3.12	4.24	3.33
logSw	− 3.21	− 3.17	− 3.3	− 3.3	− 3.77	− 3.56	− 4.38	− 3.64
Topological polar surface area	102.36	102.29	82.06	82.06	61.83	102.29	61.38	82.06
Rotatable bonds	7	7	7	7	8	7	8	8
Rigid bonds	14	14	14	14	15	14	15	15
Flexibility	0.33	0.33	0.33	0.33	0.35	0.33	0.35	0.34
Hydrogen bond donor	2	2	1	1	0	2	0	1
Hydrogen bond acceptor	7	7	6	6	5	7	5	6
Rings	2	2	2	2	2	2	2	2
Max size ring	6	6	6	6	6	6	6	6
Num charges	0	0	0	0	0	0	0	0
Total charge	0	0	0	0	0	0	0	0
Heavy atoms	23	23	22	22	23	23	24	24
Carbons atoms	17	16	16	16	18	16	18	18
Hetero atoms	6	7	6	6	5	7	6	6
Ration H/C	0.43	0.43	0.37	0.37	0.28	0.43	0.33	0.33
Lipinski violations	0	0	0	0	0	0	0	0
Solubility mg/l	12,758	13,333	11,072	11,089	7159	9022	4317	8545
Solubility forecast index	Good	Good	Good	Good	Reduced	Reduced	Reduced	Reduced
Oral_Bioavailability_VEBER	Good	Good	Good	Good	Good	Good	Good	Good
Oral_Bioavailability_EGAN;	Good	Good	Good	Good	Good	Good	Good	Good
Phospholipidosis inducer	Non-inducer	Non-inducer	Non-inducer	Non-inducer	Non-inducer	Non-inducer	Non-inducer	Non-inducer

Oral = 3,134,000 mg, SC = 3,735,000 mg), T3 (IP = 623,400 mg, IV = 165,900 mg, Oral = 2,921,000 mg, SC = 4,182,000 mg), T4 (IP = 634,100 mg, IV = 187,900 mg, Oral = 2,756,000 mg, SC = 2,797,000 mg), T5 (IP = 634,100 mg, IV = 187,900 mg, Oral = 2,756,000 mg, SC = 2,797,000 mg), T6 (IP = 654,000 mg, IV = 234,000 mg, Oral = 3,204,000 mg, SC = 3,505,000 mg), T7 (IP = 610,000 mg, IV = 94,310 mg, Oral = 1,082,000 mg, SC = 4,338,000 mg) and T8 (IP = 517,200 mg, IV 207,500 mg, Oral = 2,610,000 mg, SC = 2,383,000 mg). Henceforth, this evaluation for toxicity prediction revealed that all the phenolic derivatives possess non-toxic behavior. Table 2 indicates the toxicity prediction for all experimental molecules (from T1 to T8) using Rat Acute Toxicity GUSAR model.

Super-toxic (< 5 mg/kg), extremely toxic (5–50 mg/kg), very toxic (50–500 mg/kg), moderately toxic (500–5000 mg/kg), slightly toxic (5000–15,000 mg/kg), and practically non-toxic (> 15,000 mg/kg).

Docking results

The docking interaction of ligands from T1 to T8 with the target protein LOXL2 showed the lowest binding affinity values, especially T8 (−7.6 kcal) and T5 (−7.8 kcal), respectively, as shown in Table 3, which is an indicator of stable ligand–target complexes. All the lead compounds were docked within the most druggable site determined computationally using online server DoGSiteScorer. The residual interaction of different amino acids with T5 and T8 was viewed as shown in Figs. 2 and 3 by using Discovery Studio 4.0. The carbonyl group -CO- in compound T5 forms hydrogen bond with amino acid residue Gly330 and Gly331. Two carbon hydrogen bonds were formed with Arg 329 and Gly 331 and compound T5. Compound T8 forms three hydrogen bonds with amino acid residues Arg338, Ile 748 and Ser751. Pi-stacking and Pi-alkyl interactions in compound T8 are present between benzene rings and amino acid residue Arg 329, Ile385 and Ser726.

MD simulation evaluation

The phenolic derivatives (T5 and T8) which showed maximum binding affinity with the target protein were further selected to analyze the residual flexibility of receptor molecules. The residual deviation and fluctuations of targeted proteins of both complexes T5 and T8 are mentioned in Fig. 1. Initially, both RMSD graph lines showed an increasing trend at time 0–2500 ps as shown in Fig. 4. After that, both complexes showed different graphs fluctuations from 2500 to 5000 ps as per results indicated in Fig. 5. The T8 showed little fluctuations from 5000 to 15,000 ps, while T5 was in higher fluctuations level throughout the simulation graph. It was observed

Table 2 Toxicity prediction for all experimental molecules (from T1 to T8) using Rat Acute Toxicity GUSAR model

Route of administration	LD_{50} mg/kg							
	T1	T2	T3	T4	T5	T6	T7	T8
Intraperitoneal	656,000	637,800	623,400	634,100	634,100	654,000	610,000	517,200
Intravenous	215,400	223,400	165,900	187,900	187,900	234,000	94,310	207,500
Oral	3,081,000	3,134,000	2,921,000	2,756,000	2,756,000	3,204,000	1,082,000	2,610,000
Subcutaneous	3,824,000	3,735,000	4,182,000	2,797,000	2,797,000	3,505,000	4,338,000	2,383,000

Table 3 Binding affinity energies and root-mean-square deviation (RMSD) values obtained after docking run of ligands (T1 to T8) with target protein LOXL2

Ligand–target complex	Binding affinity	RMSD/UB	RMSD/LB	Number of hydrogen interactions	Interacting amino acid
LOXL2_T1	−7.5	0	0	2	Asp, Ile
LOXL2_T2	−6.6	0	0	4	Gly, Asp, Arg
LOXL2_T3	−6.4	0	0	3	Gly, Gly, Tyr
LOXL2_T4	−5.9	0	0	3	Gly, Gly, Arg
LOXL2_T5*	**−7.8**	**0**	**0**	**3**	**Gly, Gly, Arg**
LOXL2_T6	−6.7	0	0	2	Arg, Ile
LOXL2_T7	−6.8	0	0	3	Gly, Gly, Arg
LOXL2_T8*	**−7.6**	**0**	**0**	**3**	**Arg, Ser, Ile**

*Bold highlighted values are best-fit docked complexes based on the binding affinity values

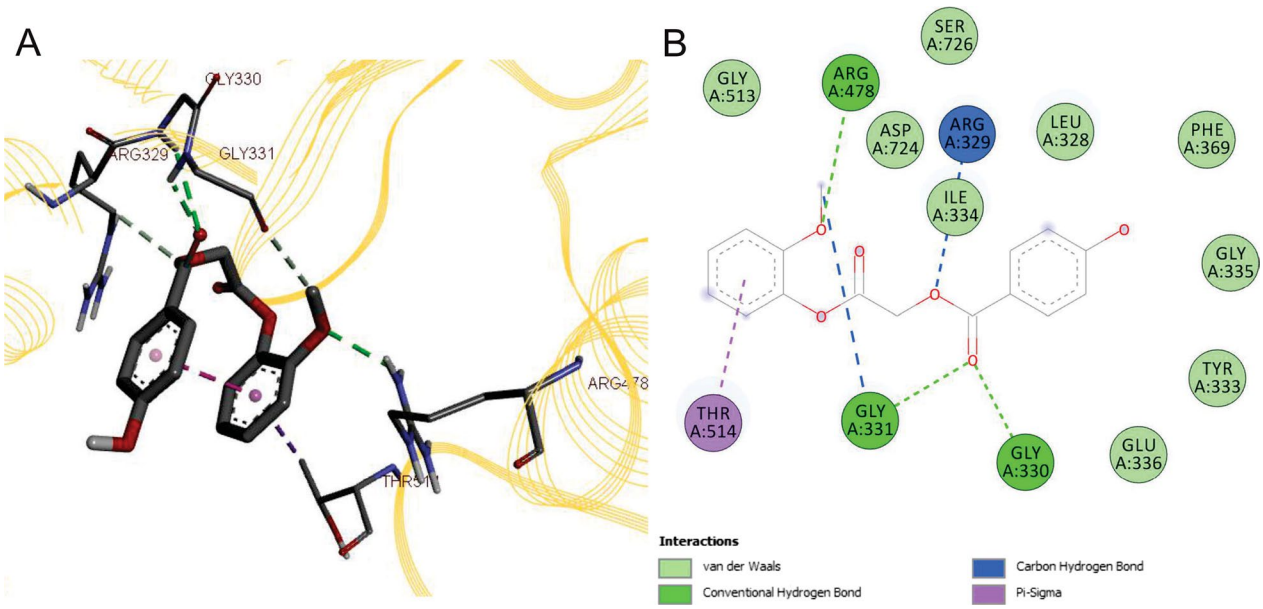

Fig. 2 **a** (3D), **b** (2D) Residual interaction of T5 in binding pocket of lysyl oxidase, T5 interacting via hydrogen bonding with amino acid Gly330 and Gly331. These interaction patterns were viewed using Discovery Studio 4.0

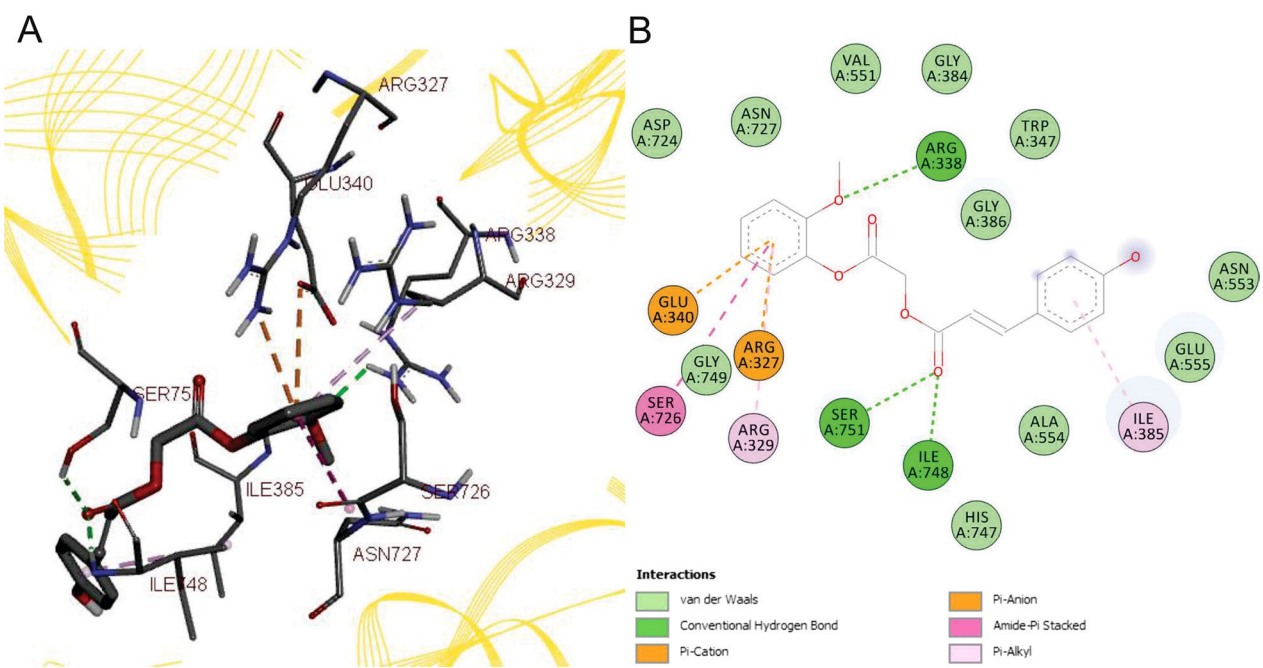

Fig. 3 **a** (3D), **b** (2D) Residual interaction of T8 in binding pocket of lysyl oxidase, T8 interacting via hydrogen bonding with amino acids Arg338, Ile 748 and Ser751. These interaction patterns were viewed using Discovery Studio 4.0

that T8 simulation graph was more stable as compared to T5 throughout the simulation time period. The compactness of protein was evaluated by radius of gyration (Rg) as mentioned in Fig. 6. The predicted results exposed that Rg value for both T5 and T8 fluctuated between 2.80 and 2.95 nm values throughout the simulation time frame 0–15,000 ps. The solvent-accessible surface area (SASA) was also observed and is depicted in Fig. 7. Results

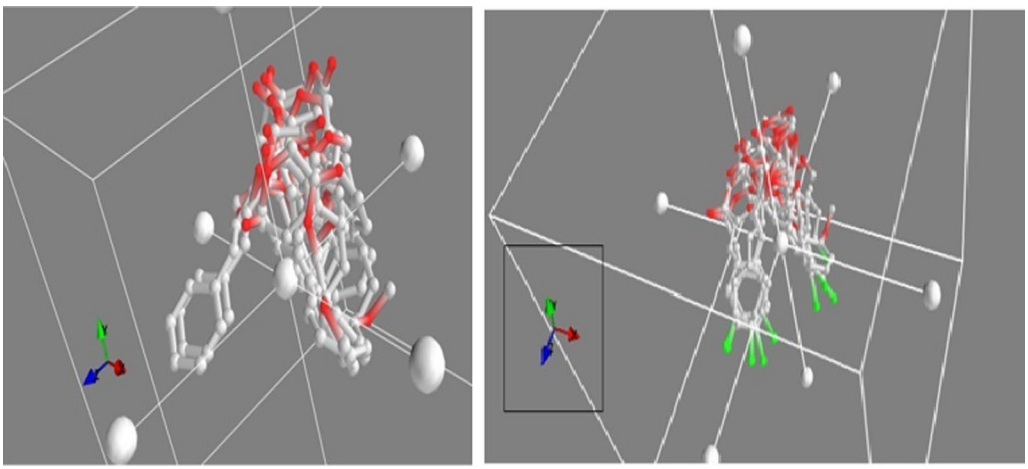

Fig. 4 Eight different structural conformations of T5 (**a**) and T8 (**b**) in binding pocket of lysyl oxidase (exhaustiveness was set at 8 before docking run)

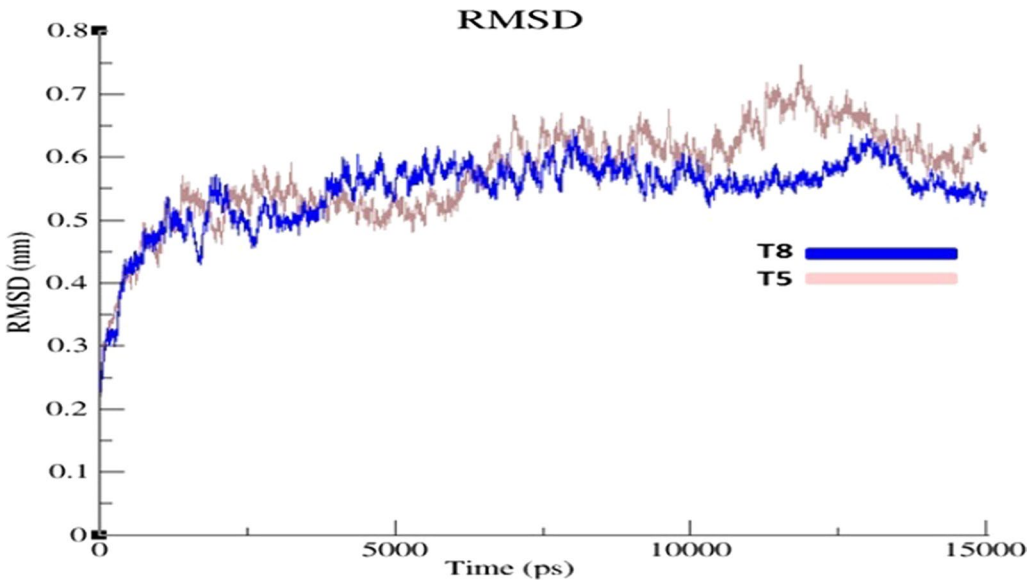

Fig. 5 RMSD graphs of T5 and T8 targeted protein at different time scales from 0 to 15,000 ps

showed that both complexes are 87 co-resided at 400 nm^2 in the simulations graphs.

Discussion

Lysyl oxidase-like 2 (LOXL2) has recently been explored as extremely pivotal protein involved in angiogenesis which results in metastasis of numerous types of cancers. Hence, LOXL2 is an exciting new target for drug development against tumor progression and its spread to distant organs. Newly synthesized derivatives of natural phenolic antioxidant guaiacol (T1 to T8) were evaluated for their potential as anti-angiogenic agents using in silico approach. The drug likeness properties and toxicity of the synthesized derivatives have also been determined. Active binding sites of LOXL2 protein were determined by online server DoGSiteScorer and lead–target interactions, and conformations of pose analysis were done by using AutoDock Vina and Discovery Studio 4.0. The GUSAR model was applied to find the toxicity and ADMET properties. On the other hand, the chemoinformatics prediction was also performed using online FAF Drug Server and Molinspiration online server.

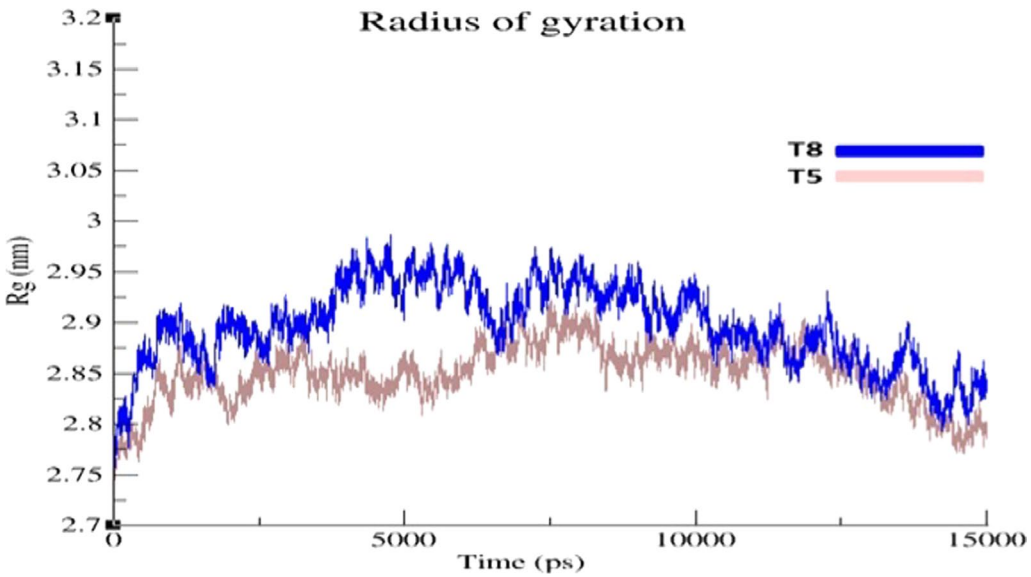

Fig. 6 Radius of gyration (Rg) graph of T5 and T8 targeted protein at different time scales from 0 to 15,000 ps

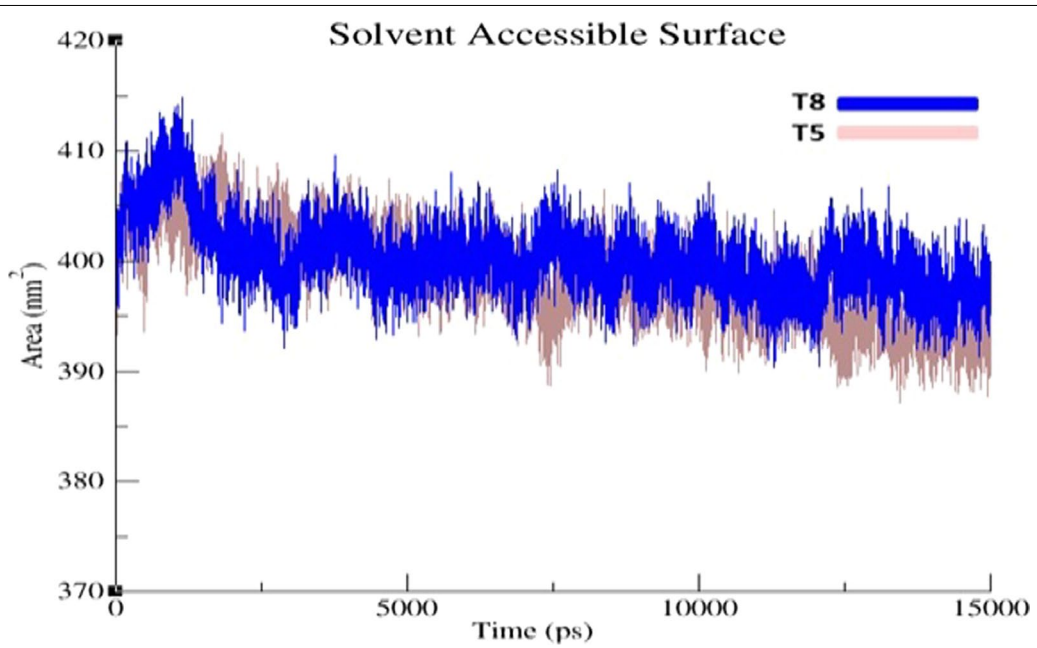

Fig. 7 Solvent-accessible surface area (SASA) graph of T5 and T8 targeted protein at different time scales from 0 to 15,000 ps

All phenolic derivatives were computationally screened for their possible rat acute toxicity prediction via four administration routes, including intraperitoneal, intravenous, oral and subcutaneous, using general unrestricted structure–activity relationship (GUSAR). The results showcased promising values for all the compounds (T1–T8). Henceforth, this evaluation for toxicity prediction revealed that all the phenolic derivatives possess non-toxic behavior.

All phenolic derivatives were screened for drug likeness properties including molecular weight, number of hydrogen bond donor atoms, number of hydrogen bond acceptor atoms, molar volume, topological polar surface area, rigid and flexible bonds and water partition coefficient,

using online chemoinformatics drug database FAF Drug Server and Molinspiration server and solubility forecast index were also determined using the same online tools for all experimental phenolic derivatives. All phenolic lead derivatives complied with rule of five, with excellent aqueous solubility and good oral bioavailability. Table 1 refers to the chemoinformatic properties of phenolic derivatives.

The PDB formats of all experimental phenolic derivatives were prepared and quality-treated to form PDBQT file using AutoDock tools. Homology model of LOXL2 was built using I-Tasser online server. Among the five proposed models, one was selected based on C Score criteria. Based on the highest confidence scores (C Scores), the best model was selected as the most stable model using I-Tasser online server. All the lead molecules (T1–T8) were docked separately against LOXL2 with exhaustiveness value = 50 using AutoDock Vina software. The predicted docked complexes were evaluated based on the lowest binding energy (kcal/mol) values, and the three-dimensional graphical depictions of all the docked complexes were accomplished by Discovery Studio 4.0. All the lead compounds were docked within the most druggable site determined computationally using online server DoGSiteScorer. The docking interaction of ligands from T1 to T8 with the target protein LOXL2 showed the lowest binding affinity values, which is an indicator of stable ligand–target complexes. The binding energy in turn determined the *in silico* inhibition of LOXL2. All the phenolic derivatives showed promising binding energies, especially T8 (− 7.6 kcal) and T5 (− 7.8 kcal), respectively, as shown in Table 3. T5 showed interaction via hydrogen bonding with amino acid Gly330 and Gly331 through hydrogen bonding as depicted in Fig. 2, while T8 interacted via hydrogen bonding with amino acids Arg 338, Ile 748 and Ser 751, as described in Fig. 3.

The best docked energy (Kcal/mol) complexes (T5 and T8) were selected for MD simulations study. This study was performed by Groningen Machine for Chemicals Simulations (GROMACS) 4.5.4 package with GROMOS 53A6 force field and water model SPC216. The topology files of receptor and ligand were created by using GROMOS 53A6 force field and online PRODRG Server. The receptor–ligand complexes were then placed in the middle of cubic box with 0.9 Å distance. The energy minimization (n steps = 50,000) was done by the steepest descent approach (1000 ps), and energy calculation was made by particle mesh Ewald (PME) method. The final MD run was adjusted to 15,000 ps with n steps 7,500,000 and analyzed using Xmgrace software. Any fluctuation in the interaction was determined by root-mean-square deviation (RMSD) and root-mean-square fluctuations (RMSF) graphs. Furthermore, to check the compactness of protein, radius of gyration (Rg), solvent-accessible surface area (SASA) (A^2) and chi, dihedral order pattern of residues were determined. The residual deviation and fluctuations of targeted proteins of both complexes T5 and T8 were obtained. Initially, both RMSD graph lines showed an increasing trend at time 0–2500 ps. After that, both complexes showed different graphs fluctuations from 2500 to 5000 ps. T8 simulation graph was more stable as compared to T5 as it showed little fluctuations from 5000 to 15,000 ps, while T5 was in higher fluctuations level throughout the simulation graph. The RMSF results reflected that both C and N-terminal lobes of targeted proteins complexes were fluctuated throughout the simulation period. The RMSF results assured the stability of both targeted protein throughout the simulation period. The compactness of protein was evaluated by radius of gyration (Rg). The predicted results exposed that Rg value for T5 and T8 was fluctuated between 2.80 and 2.95 nm values throughout the simulation time frame 0–15,000 ps. The solvent-accessible surface area (SASA) was also observed. Results showed that both complexes are 87 co-resided at 400 nm^2 in the simulations graphs.

Conclusion

The three-dimensional crystal structure of LOXL2 enzyme was successfully built using online I-Tasser server and was validated by constructing Ramachandran plot which revealed that 96% of the residues were lying in favorable quadrant of the plot. The best inhibitors of LOXL2 enzyme were screened using PyRx virtual screening tool, subsequently resulting into short listing of T5 and T8 as the finest inhibitors based on binding affinity values − 7.9 and − 8.0 kcal/mol, respectively. MD simulation studies of these best-fit lead molecules consolidated our docking outcomes and confirmed that both T5 and T8 were firmly bound in binding pocket of the target protein with minimum deviation as depicted in RMSD and RMSF graphs. The evaluations for chemoinformatic properties also derived heartening outcomes, proposing that all the phenolic derivatives were in compliance with rule of five and were having good aqueous solubility with excellent oral bioavailability and more importantly were non-inducer of phospholipidosis liver enzymes. Then afterward, toxicity prediction using GUSAR model has revealed that all the phenolic derivatives were virtually non-toxic, irrespective of their route of administration (IV, IP, oral and SC). Based upon of our results, it is proposed that T5 and T8 may act as potential inhibitors of LOXL2 enzyme and may further be evaluated in wet laboratory. It was further proposed that these *in silico* tools may be used to screen new compounds using different computational models.

Abbreviations
LOXL2: Lysyl oxidase-like 2; GUSAR: General unrestricted structure–activity relationship; ADMET: Absorption, distribution, metabolism, elimination, toxicity; LOX: Lysyl oxidase; ECM: Extracellular matrix; HNSCC: Head and neck squamous cell carcinoma; IP: Intraperitoneal; IV: Intravenous; SC: Subcutaneous; C Scores: Confidence scores; MD: Molecular dynamics.

Supplementary Information

The online version contains supplementary material available at https://doi.org/10.1186/s43094-022-00422-8.

Additional file 1: Docking interactions of all the phenolic derivatives with LOXL2. **Figure S1** Residual interaction of T1 in binding pocket of Lysyl Oxidase, T1 interacting via hydrogen bonding with amino acid Asp724 and Ile748. These interaction patterns were viewed using Discovery Studio 4.0. **Figure S2**. Residual interaction of T2 in binding pocket of Lysyl Oxidase, T2 interacting via hydrogen bonding with amino acid Gly331, Arg748 and Asp724. These interaction patterns were viewed using Discovery Studio 4.0. **Figure S3**. Residual interaction of T3 in binding pocket of Lysyl Oxidase, T3 interacting via hydrogen bonding with amino acid Gly330, Gly331 and Tyr333. These interaction patterns were viewed using Discovery Studio 4.0. **Figure S4**. Residual interaction of T4 in binding pocket of Lysyl Oxidase, T4 interacting via hydrogen bonding with amino acid Gly330, Gly331 and Arg478. These interaction patterns were viewed using Discovery Studio 4.0. **Figure S5**. Residual interaction of T6 in binding pocket of Lysyl Oxidase, T6 interacting via hydrogen bonding with amino acid Arg327 and Ile748. These interaction patterns were viewed using Discovery Studio 4.0. **Figure S6**. Residual interaction of T7 in binding pocket of Lysyl Oxidase, T7 interacting via hydrogen bonding with amino acid Gly330, Gly331 and Arg478. These interaction patterns were viewed using Discovery Studio 4.0.

Acknowledgements
All authors are highly acknowledged for their contributions.

Author contributions
MTA and NR deigned, supervised and performed computational studies. SU, AU and ZA reviewed and helped in the analysis. MA performed docking studies/analysis and helped in manuscript preparation. All authors read and approved the final manuscript.

Funding
Not applicable.

Availability of data and materials
All data and materials are available upon request.

Declarations

Ethical approval and consent to participate
Not applicable.

Consent for publication
Not applicable.

Competing interests
There is no conflict of interest regarding publication of the current research work.

Author details
[1]Department of Pharmacy, COMSATS University Islamabad, Abbottabad Campus, Islamabad 22060, Pakistan. [2]Margalla College of Pharmacy, Margalla Institute of Health Sciences, Rawalpindi, Pakistan. [3]Department of Pharmacology, Riphah Institute of Pharmaceutical Sciences, Riphah International University, Islamabad, Pakistan. [4]Department of Chemistry, Allama Iqbal Open University, Islamabad, Pakistan. [5]Department of Pharmaceutical Chemistry, Riphah Institute of Pharmaceutical Sciences, Riphah International University, Islamabad, Pakistan.

Received: 30 August 2021 Accepted: 31 May 2022
Published online: 11 June 2022

References

1. Fidler IJ (2003) The pathogenesis of cancer metastasis: the'seed and soil'hypothesis revisited. Nat Rev Cancer 3(6):453–458
2. Folkman J. Angiogenesis. In: Biology of endothelial cells;1984. Springer. p. 412–28.
3. Kagan HM, Li W (2003) Lysyloxid-+ase: properties, specificity, and biological roles inside and outside of the cell. J Cell Biochem 88(4):660–672
4. Kim YM, Kim EC, Kim Y (2011) The human lysyl oxidase-like 2 protein functions as an amine oxidase toward collagen and elastin. Mol Biol Rep 38(1):145–149
5. Erler J, Le Q, Giaccia AJ (2006) 88: lysyl oxidase is essential for hypoxia-induced metastasis. Int J Radiat Oncol Biol Phys 66(3):S50
6. Kirschmann DA (2002) A molecular role for lysyl oxidase in breast cancer invasion. Cancer Res 62(15):4478–4483
7. Baker A (2013) Lysyl oxidase enzymatic function increases stiffness to drive colorectal cancer progression through FAK. Oncogene 32(14):1863–1868
8. Baker AM (2011) The role of lysyl oxidase in SRC-dependent proliferation and metastasis of colorectal cancer. J Natl Cancer Inst 103(5):407–424
9. Lapointe J (2004) Gene expression profiling identifies clinically relevant subtypes of prostate cancer. Proc Natl Acad Sci USA 101(3):811–816
10. Barry-Hamilton V (2010) Allosteric inhibition of lysyl oxidase-like-2 impedes the development of a pathologic microenvironment. Nat Med 16(9):1009–1017
11. Rückert F (2010) Functional analysis of LOXL2 in pancreatic carcinoma. Int J Colorectal Dis 25(3):303–311
12. Akiri G (2003) Lysyl oxidase-related protein-1 promotes tumor fibrosis and tumor progression in vivo. Cancer Res 63(7):1657–1666
13. Tungmunnithum D (2018) Flavonoids and other phenolic compounds from medicinal plants for pharmaceutical and medical aspects: an overview. Medicines 5(3):93
14. Weng CJ, Yen GC (2012) Flavonoids, a ubiquitous dietary phenolic subclass, exert extensive in vitro anti-invasive and in vivo anti-metastatic activities. Cancer Metastasis Rev 31:256
15. Fortes C (2012) Evaluation of the anti-angiogenic potential of hydroxytyrosol and tyrosol, two bio-active phenolic compounds of extra virgin olive oil, in endothelial cell cultures. Food Chem 134(1):134–140
16. López-Jiménez A (2013) Anti-angiogenic properties of carnosol and carnosic acid, two major dietary compounds from rosemary. Eur J Nutr 52(1):85–95
17. Wang N, Wang ZU, Mo SL, Loo TY, Wang DM, Luo HB, Yang DP, Chen YL, Shen JG, Chen JP (2012) Ellagic acid, a phenolic compound, exerts anti-angiogenesis effects via VEGFR-2 signaling pathway in breast cancer. Breast Cancer Res Treat 134(3):943–955
18. Aqeel MT (2018) Antihyperlipidemic studies of newly synthesized phenolic derivatives: in silico and in vivo approaches. Drug Des Dev Ther 12:2443
19. Volkamer A, Kuhn D, Rippmann F, Rarey M (2012) DoGSiteScorer: a web server for automatic binding site prediction, analysis and druggability assessment. Bioinformatics 28(15):2074–2075
20. Trott O, Olson AJ (2010) AutoDockVina: improving the speed and accuracy of docking with a new scoring function, efficient optimization, and multithreading. J Comput Chem 31(2):455–461
21. Discovery Studio Visualizer Software, Version 4.0. (2012). http://www.accelrys.com.
22. Lagunin A, Zakharov A, Filimonov D, Poroikov V (2011) QSAR modelling of rat acute toxicity on the basis of PASS prediction. Mol Inform 30(2–3):241–250
23. LagorceD SO, Baell JB, Miteva MA, Villoutreix BO (2015) FAF-Drugs3: a web server for compound property calculation and chemical library design. Nucleic Acids Res 43(W1):W200–W207
24. Cheminformatics M. Molinspiration Cheminformatics. 2013.
25. Roy A, Kucukural A, Zhang Y (2010) I-TASSER: a unified platform for automated protein structure and function prediction. Nat Protoc 5(4):725–738

26. Morris GM, Huey R, Lindstrom W, Sanner MF, Belew RK, Goodsell DS, Olson AJ (2009) AutoDock4 and AutoDockTools4: Automated docking with selective receptor flexibility. J Comput Chem 30(16):2785–2791
27. Pronk S, Pall S, Schulz R, Larsson P, Bjelkmar P, Apostolov R, Shirts MR, Smith JC, Kasson PM, Spoel DVD, Hess B. GROMACS 4.5: a high-throughput and highly parallel open source molecular simulation toolkit. Bioinformatics;2013. p. btt055.
28. OostenbrinkC VA, Mark AE, Gunsteren WFV (2004) A biomolecular force field based on the free enthalpy of hydration and solvation: the GROMOS force-field parameter sets 53A5 and 53A6. J Comput Chem 25(13):1656–1676
29. SchuÈttelkopf AW, Van Aalten DM (2004) PRODRG: a tool for high-throughput crystallography of protein–ligand complexes. Acta Crystallogr Sect D Biol Crystallogr 60(8):1355–1363
30. Wang H, Dommert F, Holm C (2010) Optimizing working parameters of the smooth particle mesh Ewald algorithm in terms of accuracy and efficiency. J Chem Phys 133(3):034117
31. Turner PJ. XMGRACE, Version 5.1.19. Center for Coastal and Land-Margin Research, Oregon Graduate Institute of Science and Technology, Beaverton; 2005.
32. Mittal L, Srivastava M, Kumari A, Tonk RK, Awasthi A, Asthana S (2021) Interplay among structural stability, plasticity, and energetics determined by conformational attuning of flexible loops in PD-1. J Chem Inf Model 61(1):358–384

Publisher's Note